

Transient Behaviour of Grounding System in a Two-Layer Soil Using the Transmission Line Theory

DOI 10.7305/automatika.2014.12.497
UDK 621.315.5.09:631.437
IFAC 4.3.2; 1.1.9

Original scientific paper

The present work deals with modeling of the transient behavior of grounding systems in the presence of layered media. A simple and efficient Transmission Line (TL) model featuring the use of the Finite Difference Time Domain (FDTD) is proposed. The proposed approach easily accounts for the influence of semi-infinite media (soil or air) and imposes conditions at the interfaces. The TL model is verified through the direct solution of the Maxwell's equations in the time domain by means of the FDTD method. Some illustrative computational examples addressing some engineering applications stemming from industry are given in the paper.

Key words: Transient response, Grounding system, Transmission line theory, Maxwell's equation's approach, Two-layer soil, Finite difference time domain (FDTD) method

Tranzijentni odziv uzemljivačkog sustava u dvoslojnom tlu primjenom teorije prijenosnih linija. U radu se razmatra modeliranje tranzijentnog odziva uzemljivačkog sustava u prisutnosti slojevitih sredina. Predložen je jednostavan i efikasan model prijenosne linije uz upotrebu metode prijenosnih linija u vremenskom području. U okviru predloženog pristupa lako se uzima u obzir utjecaj polubeskonačnih sredina (tlo ili zrak) te postavljaju uvjeti na granici sredina. Model prijenosne linije verificira se direktnim rješenjem Maxwellovih jednažbi u vremenskom području primjenom metode konačnog diferencija u vremenskom području. U radu se daju neki ilustrativni računalni primjeri koji se odnose na neke inženjerske primjene proizašle iz prakse.

Ključne riječi: Tranzijentni odziv, uzemljivački sustav, teorija prijenosnih linija, pristup preko Maxwellovih jednažbi, dvoslojno tlo, metoda konačnih diferencija u vremenskom području

The principal task of grounding systems is to ensure the safety of personnel and prevent damage of installations and equipment. Defect on grounding systems may cause operation error, malfunction and destruction of components in electric and electronic systems connected to the grounding systems. During a short circuit or lightning discharge, the assessment of fault currents in the grounding systems is rather important task, as these currents cause an increase of ground potential and related high intensity electromagnetic fields. The increase in ground potential is dangerous for the technical staff inside the substation, while the radiated fields may affect the measuring equipment required for the control and management of the power network.

To analyze the behaviour of grounding systems under lightning regime, several models for transient analysis of grounding systems were developed. Thus, the problem of the grounding is usually treated by means of the Moment Method (MoM) [1], Finite Element Method (FEM) [2-3] and Finite Difference Method (FDM) [4-5]. Recently, an

approach based on voltage propagation equation and Finite Difference Time Domain (FDTD) solution method has been reported in [5].

The model proposed in this work has been developed as an extension of the homogeneous soil model, based on the Transmission Line (TL) theory and the FDTD solution method. The two-layer soil effects are taken into account by means of the concept of apparent resistivity.

An alternative approach used in this work for the transient analysis of grounding systems is the FDTD solution of Maxwell's equations in inhomogeneous media (layers of soil, air and the conductors of the ground).

First, a rather simple case of a single horizontal buried electrode is considered. What follows up is the configuration of a grounding grid. Some illustrative computational examples are presented throughout the paper.

1 TRANSMISSION LINE APPROACH

The use of numerical models leads to rigorous solutions, but at the same time very often difficult to imple-

ment and use by engineers. When the grounding systems are composed entirely of wire conductors as shown in the Figure 1, a simple model developed using the TL theory could be used.

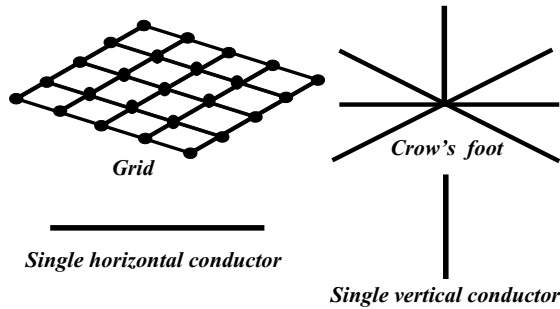


Fig. 1. Representation of grounding by a single conductor or by interconnected conductors

It is worth mentioning that TL has been already used to simulate the transient behaviour of counterpoise wire. Transient behaviour of counter-poise wire is similar overhead transmission lines. TL approach for modeling transient behaviour of grounding systems can be carried out in either time or frequency domain, but it is easier to include soil ionization in the time domain.

Using the TL approach enables one to predict surge propagation delay which is quite important for large grounding systems. Furthermore, the computational cost required for TL approach is significantly less compared to the requirements posed by the full wave model.

2 TRANSIENT ANALYSIS VIA TL EQUATIONS

The transient behaviour of the grounding conductors can be simulated using the TL equations:

$$\frac{\partial v(x, t)}{\partial x} + Ri(x, t) + L \frac{\partial i(x, t)}{\partial t} = 0, \quad (1)$$

$$\frac{\partial i(x, t)}{\partial x} + Gv(x, t) + C \frac{\partial v(x, t)}{\partial t} = 0, \quad (2)$$

where $v(x, t)$, and $i(x, t)$ are the unknown distributed voltage and current along the grounding wire. R is the per-unit length series resistance. L , G and C are the effective per-unit length inductance, conductance and capacitance of the conductor, respectively.

The per unit lines parameters of buried vertical and horizontal electrodes can be calculated by using E. D. Sunde [6] or Y. Liu [7] formulas, respectively.

Figure 2 shows the grounding system composed from simple conductors and it is considered as a graph. Note

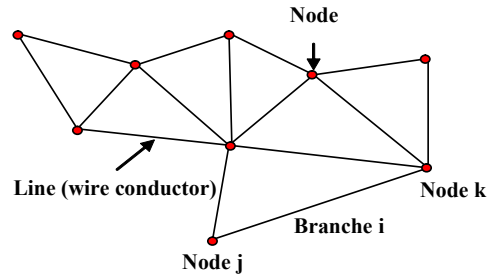


Fig. 2. Meshed network with N uniform transmission Lines and m nodes

that the branches of this graph are the wires (conductors) interconnected by nodes.

The transient behaviour of grounding systems in the lightning regime is governed by the following matrix equation:

$$[A] [X] = [B], \quad (3)$$

obtained by discretizing the TL equations based on FDTD method and the application of Kirchhoff's laws in all nodes of meshed network.

Not that the system matrix is composed from two sub matrices, as follows:

$$[A] = \begin{bmatrix} [A_1] \\ [A_2] \end{bmatrix}, \quad (4)$$

where $[A_1]$ is the matrix of the network topology that accounts for the propagation on the line segments; $[A_2]$ is the sub matrix obtained by applying the Kirchhoff's laws (KCL and KVL) for junctions (terminations' and interconnections' networks) [2].

Furthermore $[X]$ denotes the vector of unknown currents and voltages in all nodes while $[B]$ stands for the source vector.

2.1 Quadruple representation of the line in time domain

For a conductor of length L , following notation is used:

$$(v)_k^n \equiv v((k - 1) \Delta x, n \Delta t), \quad (5)$$

$$(i)_k^n \equiv i((k - 1/2) \Delta x, (n + 1/2) \Delta t), \quad (6)$$

$$l = (k_{max} - 1) \Delta x,$$

$$t_{max} = n_{max} \Delta t.$$

The related FDTD scheme is shown in Fig. 3.

Discretizing the TL equations (1) and (2) using the formalism of the FDTD method one the following discrete

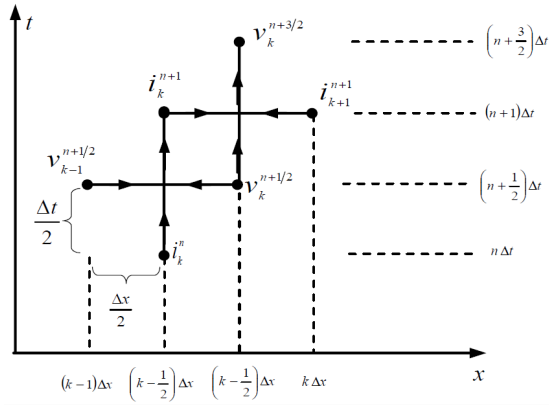


Fig. 3. The relation between the spatial and temporal discretizations to achieve second order accuracy in the discretization of the derivatives

equations are obtained:

$$[v_k^n] = \left(\frac{C}{\Delta t} - \frac{G}{2}\right)^{-1} \left[\left(\frac{C}{\Delta t} - \frac{G}{2}\right) [v_k^{n-1}] - \left(\frac{[i_k^{n-1}] - [i_{k-1}^{n-1}]}{\Delta x}\right) \right], \tag{7}$$

$$[i_k^n] = \left(\frac{L}{\Delta t} + \frac{R}{2}\right)^{-1} \left[\left(\frac{L}{\Delta t} - \frac{R}{2}\right) [i_k^{n-1}] - \left(\frac{[v_{k+1}^n] - [v_k^n]}{\Delta x}\right) \right]. \tag{8}$$

Note that the two ends of the line are defined in terms of the voltage nodes. Figure 4 shows a quadruple representation of the line in the time domain:

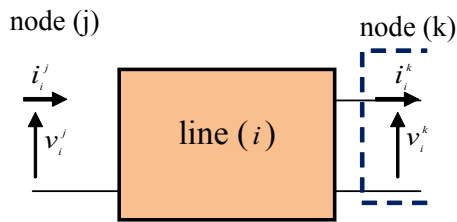


Fig. 4. Quadruple representation in time domain of the single branch

Two fictitious nodes of currents at the two ends of line are formed (for $X = 0$ and $X = L$).

Setting:

$$v_1^n = (v(0))^n \text{ and } i_0^{n-1/2} = (i(0))^{n-1/2} \text{ for } x = 0, \tag{9}$$

$$v_{k_{max}+1}^n = (v(L))^n \text{ and } i_{k_{max}+1}^{n-1/2} = (i(L))^{n-1/2} \text{ for } x = L, \tag{10}$$

and by assuming the approximations:

$$(i(0))^{n-1/2} = \frac{(i(0))^n + (i(0))^{n-1}}{2}, \tag{11}$$

$$(i(L))^{n-1/2} = \frac{(i(L))^n + (i(L))^{n-1}}{2}, \tag{12}$$

the equation corresponding to the first end of the line $k = 1$ ($x = 0$) is obtained:

$$\left[\frac{C}{\Delta t} + \frac{G}{2}\right] [v^n(0)] - \frac{[i^n(0)]}{\Delta x} = \left[\frac{C}{\Delta t} - \frac{G}{2}\right] [v^{n-1}(0)] - \frac{[i_1^{n-1}]}{(\Delta x/2)} + \frac{[i^{n-1}(0)]}{(\Delta x)}. \tag{13}$$

Furthermore, the equation corresponding to second end of the line is $k = k_{max} + 1$ ($x = L$):

$$\left[\frac{C}{\Delta t} + \frac{G}{2}\right] [v^n(L)] - \frac{[i^n(L)]}{\Delta x} = \left[\frac{C}{\Delta t} - \frac{G}{2}\right] [v^{n-1}(L)] + \frac{[i_{k_{max}}^{n-1/2}]}{(\Delta x/2)} - \frac{[i^{n-1}(L)]}{(\Delta x)}. \tag{14}$$

Finally, one derives the quadruple time domain representation given by:

$$\begin{bmatrix} \frac{C}{\Delta t} + \frac{G}{2} & -\frac{1}{\Delta x} & 0 & 0 \\ 0 & 0 & \frac{C}{\Delta t} + \frac{G}{2} & \frac{1}{\Delta x} \end{bmatrix} \begin{bmatrix} (v(0))^n \\ (i(0))^n \\ (v(L))^n \\ (i(L))^n \end{bmatrix} = \begin{bmatrix} \left[\frac{C}{\Delta t} - \frac{G}{2}\right] [v^{n-1}(0)] - \frac{[i_1^{n-1}]}{(\Delta x/2)} + \frac{[i^{n-1}(0)]}{(\Delta x)} \\ \left[\frac{C}{\Delta t} - \frac{G}{2}\right] [v^{n-1}(L)] + \frac{[i_{k_{max}}^{n-1/2}]}{(\Delta x/2)} - \frac{[i^{n-1}(L)]}{(\Delta x)} \end{bmatrix}. \tag{15}$$

Having numbered all the wires (branches) and nodes of the graph representation (Figure 2) of the grounding system, the sub matrix $[A_1]$ is obtained while writing for each line the relation (15). The contribution of the line l (between nodes j and k) as shown on Fig. 2 in the sub matrix $[A_1]$ can be written:

$$\begin{bmatrix} \dots & \dots & \dots & \dots & \dots & \dots \\ \vdots & \frac{C}{\Delta t} + \frac{G}{2} & -\frac{1}{\Delta x} & 0 & 0 & \vdots \\ \vdots & 0 & 0 & \frac{C}{\Delta t} + \frac{G}{2} & \frac{1}{\Delta x} & \vdots \\ \vdots & \vdots & \vdots & \vdots & \vdots & \vdots \\ \dots & \dots & \dots & \dots & \dots & \dots \end{bmatrix} \begin{bmatrix} \vdots \\ v_i^j \\ v_i^k \\ v_l^k \\ i_l^k \\ \vdots \end{bmatrix}, \tag{16}$$

where j and k subscribe the extremities of the conductor and l represents the branch.

Furthermore, the sub matrix $[A_2]$ is developed using the Kirchhoff's laws (KVL and KCL) at each node m of the grounding system [8]

$$\sum_{j=1}^{NL} ([Y_j^m][v_j^m] + [Z_j^m][i_j^m]) - [P^m(v_j^m, i_j^m)] = 0, \quad (17)$$

where $[Y_j^m]$ represents resultant matrices from the application of Kirchhoff's laws (KVL and KCL) in the m^{th} network, which can contain the numerical values 0, 1, -1 and admittances values according to the topology of the network, $[Z_j^m]$ is related to resultant matrices from the application of Kirchhoff's laws (KVL and KCL) in the m^{th} network, which can contain the numerical values 0, 1, -1 and impedances values according to the topology of the network, $[P^m]$ is the vector of current or voltage localized sources.

Finally, the submatrix $[B]$ is composed of two sub vectors $[B_1]$ and $[B_2]$, as follows:

$$[B] = \begin{bmatrix} [B_1] \\ [B_2] \end{bmatrix} \quad (18)$$

Note that the sub vector $[B_1]$ is constructed from the second member of the matrix system (15), the sub vector $[B_2]$, contains the equivalent Thévenin and/or Norton sources (localized network) in one or more node.

3 TRANSIENT ANALYSIS VIA MAXWELL'S EQUATIONS

Assuming neither anisotropic nor dispersive medium in the domain of interest, the Maxwell's equations in the Cartesian coordinates are:

$$\nabla \times \vec{E}(t, r) = -\frac{\partial \vec{B}(t, r)}{\partial t}, \quad (19)$$

$$\nabla \times \vec{H}(t, r) = \vec{J}(t, r) + \epsilon \frac{\partial \vec{E}(t, r)}{\partial t}, \quad (20)$$

where \vec{E} is the electric field; \vec{H} is the magnetic field while ρ stands for charge density; ϵ is the permittivity; μ permeability and σ is the conductivity.

The domain of interest is a rectangular-parallelepiped, referred to as the Yee cell [9]. Figure 5 shows the cell with the configuration of electric and magnetic fields considered to be constant within the cell.

Using this cell configuration (Fig. 5) and space-time finite difference discretisation of (19) and (20) yields:

$$E_x^{n+1} \left(i + \frac{1}{2}, j, k \right) = A \cdot E_x^n \left(i + \frac{1}{2}, j, k \right) + B \cdot \begin{bmatrix} \frac{H_z^{n+\frac{1}{2}}(i+\frac{1}{2}, j+\frac{1}{2}, k) - H_z^{n+\frac{1}{2}}(i+\frac{1}{2}, j-\frac{1}{2}, k)}{\Delta y} \\ -\frac{H_y^{n+\frac{1}{2}}(i+\frac{1}{2}, j, k+\frac{1}{2}) - H_y^{n+\frac{1}{2}}(i+\frac{1}{2}, j, k-\frac{1}{2})}{\Delta z} \end{bmatrix}, \quad (21)$$

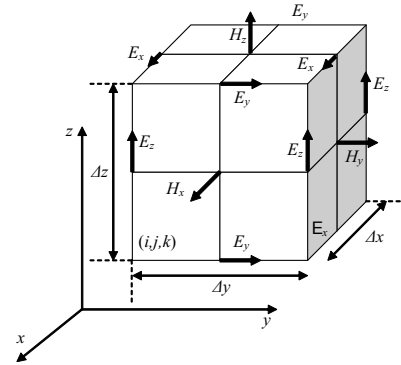


Fig. 5. Configuration of electric and magnetic fields in cell

$$H_x^{n+\frac{1}{2}} \left(i, j + \frac{1}{2}, k + \frac{1}{2} \right) = H_x^{n-\frac{1}{2}} \left(i, j + \frac{1}{2}, k + \frac{1}{2} \right) - \frac{\Delta t}{\mu} \cdot \begin{bmatrix} \frac{E_z^n(i, j+1, k+\frac{1}{2}) - E_z^n(i, j, k+\frac{1}{2})}{\Delta y} \\ -\frac{E_y^n(i, j+\frac{1}{2}, k+1) - E_y^n(i, j+\frac{1}{2}, k)}{\Delta z} \end{bmatrix}, \quad (22)$$

where A and B are given by:

$$A = \frac{1 - \frac{\sigma \cdot \Delta t}{2 \cdot \epsilon}}{1 + \frac{\sigma \cdot \Delta t}{2 \cdot \epsilon}}, B = \frac{\frac{\Delta t}{\epsilon}}{1 + \frac{\sigma \cdot \Delta t}{2 \cdot \epsilon}}. \quad (23)$$

Other electromagnetic field components are deduced by a simple circular permutation of the space variables.

4 THIN WIRE REPRESENTATION

Analysis of the frequency content of the lightning wave shows that the maximum frequency does not exceed a few MHz ($f_{max} < 10\text{MHz}$). In this case the cell size is larger than the section of the conductors of the buried electrode. Thus, a simplified model proposed by Umashankar et al. is used [10]. This method avoids the high computation time and is based on the thin wire representation by correcting the adjacent magnetic fields of the wire according to its radius [11-12]. The thin wire is defined as a conductive wire with radius smaller than the size of a cell in the FDTD simulation. The approximation is outlined in this section for the sake of completeness.

4.1 Modification of permittivity and permeability

In many engineering applications, such as antennas and grounding systems, it is necessary to model electrically thin conducting cylinders which means that the radiuses r_0 of such conducting structures are smaller than the smallest Yee's cell dimensions. Thus, a special formulation must be implemented in order to correctly model the radii. There are two basic approaches: a) correction of tangential magnetic field components [10] and b) correction of the parameters ϵ , σ and μ for the field components near the conductor as depicted in Fig. 6 [10].

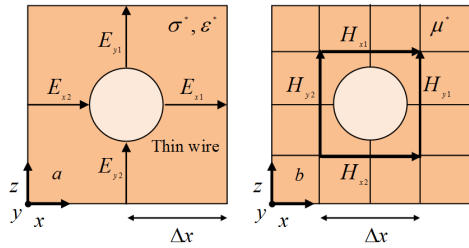


Fig. 6. A thin wire transversal section and four adjacent cells (a) four radial electric field components near the wire; (b) four magnetic field components involving the wire

As the latter methodology is appropriate for conductive media containing metallic thin wires it used in this work, as well. The corrected values of the parameters σ_s , ϵ_s and μ_s used for updating the field components shown in figure 6 are given by [10]:

$$\sigma^* = \sigma_s \frac{\ln(1/0.23)}{\ln(\Delta x/r_0)}, \quad (24)$$

$$\epsilon_s^* = \epsilon_s \frac{\ln(1/0.23)}{\ln(\Delta x/r_0)}, \quad (25)$$

$$\mu_s^* = \mu_s \frac{\ln(\Delta x/r_0)}{\ln(1/0.23)}, \quad (26)$$

where r_0 is the desired radius ($r_0 < \Delta x/2$), σ , ϵ_s and μ_s are the real media parameters, Δx is the edge dimension of a cubic Yee's cell and σ^* , ϵ_s^* and μ_s^* are the corrected values of the specified parameters for the proper field components.

5 THE AIR-GROUND INTERFACE

Contour Integral Approach [13], derived from Maxwell's equations in integral form is used to account for the air-ground interface. For the problems including inhomogeneous media and a non-uniform spatial discretization, Maxwell's equations in their integral form are convenient to use [13].

Fig. 7 shows a grid of FDTD discretization of the air-ground interface.

From Ampere's law(Maxwell's equation in) integral form:

$$\oint_l \vec{H} \cdot d\vec{l} = \iint_s \left(\sigma \vec{E}_x + \epsilon \frac{\partial \vec{E}_x}{\partial t} \right) d\vec{s}, \quad (27)$$

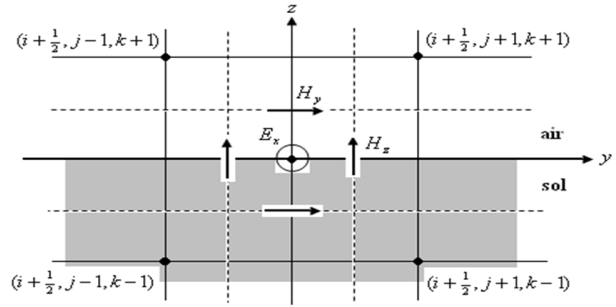


Fig. 7. Consideration of air-ground interface by the "the contour integral approach" method

it follows:

$$\begin{aligned} \oint_l \vec{H} d\vec{l} = & \left[H_z^{n+\frac{1}{2}}(i+1/2, j+1/2, k) \right. \\ & - H_z^{n+\frac{1}{2}}(i+1/2, j-1/2, k) \Big] \Delta z \\ & + \left[H_y^{n+\frac{1}{2}}(i+1/2, j, k-1/2) \right. \\ & \left. - H_y^{n+\frac{1}{2}}(i+1/2, j, k+1/2) \right] \Delta y, \quad (28) \end{aligned}$$

$$\begin{aligned} \iint_s \left(\sigma \vec{E}_x + \epsilon \frac{\partial \vec{E}_x}{\partial t} \right) d\vec{s} = & \frac{\Delta y \Delta z}{2} \epsilon_0 \frac{\partial E_x}{\partial t} \\ & + \frac{\Delta y \Delta z}{2} \left(\epsilon_s \frac{\partial E_x}{\partial t} + \sigma_s E_x \right). \quad (29) \end{aligned}$$

Combining (28) and (29) yields:

$$\begin{aligned} E_x^{n+1}(i+1/2, j, k) = & \frac{K}{N} \cdot E_x^n(i+1/2, j, k) \\ & + \frac{1}{N \cdot \Delta y} \cdot \left[H_z^{n+\frac{1}{2}}(i+1/2, j+1/2, k) \right. \\ & \left. - H_z^{n+\frac{1}{2}}(i+1/2, j-1/2, k) \right] \\ & - \frac{1}{N \cdot \Delta z} \left[H_y^{n+\frac{1}{2}}(i+1/2, j, k+1/2) \right. \\ & \left. - H_y^{n+\frac{1}{2}}(i+1/2, j, k-1/2) \right], \quad (30) \end{aligned}$$

where

$$\begin{aligned} K &= \frac{1}{2\Delta t} (\epsilon_0 + \epsilon_s) - \frac{\sigma_s}{4}, \\ N &= \frac{1}{2\Delta t} (\epsilon_0 + \epsilon_s) + \frac{\sigma_s}{4}. \quad (31) \end{aligned}$$

The other field components can be derived in the similar manner. The same expression is used to ensure the passage between the two conductive layers of the soil.

6 THE LATTICE TRUNCATION CONDITIONS

Observing the FDTD equations (22 and 23), it is clear that it is necessary to truncate the calculation domain, as long as, for open domains, they require an infinite lattice.

In order to achieve this goal, absorbing regions must be implemented at the domain's limits, simulating the wave propagation to infinitely long distances. This avoids non-natural reflections into the domain under analysis. In this context, the absorbing conditions delayed [14] formulation has been employed.

7 NUMERICAL RESULTS

In order to verify the TL approach in two-layer soil using the concept of apparent resistivity [15], the transient behaviours of horizontal grounding systems is simulated and compared with the direct solution of the Maxwell's equations in two-layer soil. In the calculations carried out via TL approach, the two-layer soil are homogenized and replaced by a single resistivity called apparent resistivity. The solution of Maxwell's equations by FDTD is performed by taking into account the variation in conductivity between the conductive layers of the soil.

7.1 Two-Layer Soil Apparent Resistivity

A resistivity determination using the Wenner-method results in an apparent resistivity which is a function of the electrode separation.

The apparent resistivity ρ_a is given by:

$$\rho_a = \rho_1 \left(1 + 4 \sum_{i=1}^{\infty} \frac{K^n}{\sqrt{1 + (2n \frac{h}{a})^2}} - \frac{K^n}{\sqrt{4 + (2n \frac{h}{a})^2}} \right), \tag{32}$$

where h is the first layer height, while ρ_1 and ρ_2 is the first and second layer resistivity, respectively. n et a

A two-layer soil can be represented by an upper layer soil of a finite depth above a lower layer of infinite depth. The abrupt change in resistivity at the boundaries of each soil layer can be described by means of a reflection factor, K , is defined by (31) [15].

$$K = \frac{\rho_2 - \rho_1}{\rho_2 + \rho_1}. \tag{33}$$

7.2 Electrode in two-layer stratified soil

Figure 8 shows an electrode buried horizontally at depth of 0.4 m from the soil-air interface. The radius of the conductor is 7 mm and its length is 20 m, while the height of the upper layer is of 2 m. The electrode is excited by a voltage source given by double-exponential function: $V(t) = 30(e^{-45099t} - e^{-9022879t})$ KV.

Physical constants (ϵ, ρ) of the medium are shown in the Fig. 8.

Figures 9 to 12 show transient currents and voltages induced on the horizontal grounding electrode determined by TL and Maxwell's equations approaches, respectively.

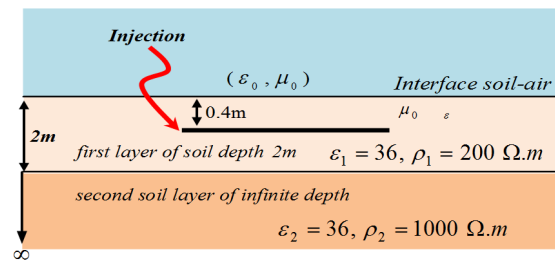


Fig. 8. Horizontal grounding conductors in two layer soil

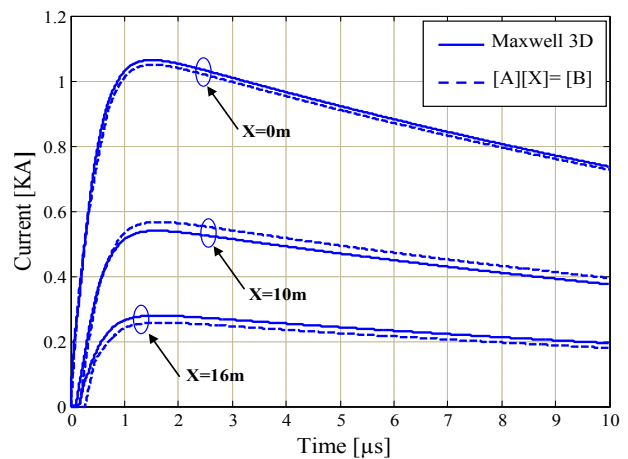


Fig. 9. Transient currents at different points for the horizontal grounding wire

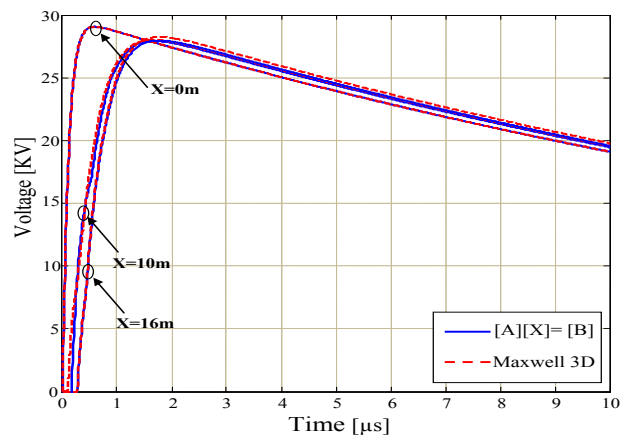


Fig. 10. Transient voltages at different points for the horizontal grounding wire

From the presented numerical results in figures 9 and 10 it can be observed that the two approaches provide similar results in both amplitude and general shape. The concept of apparent resistivity is confirmed by solving Maxwell's equations via FDTD, as well.

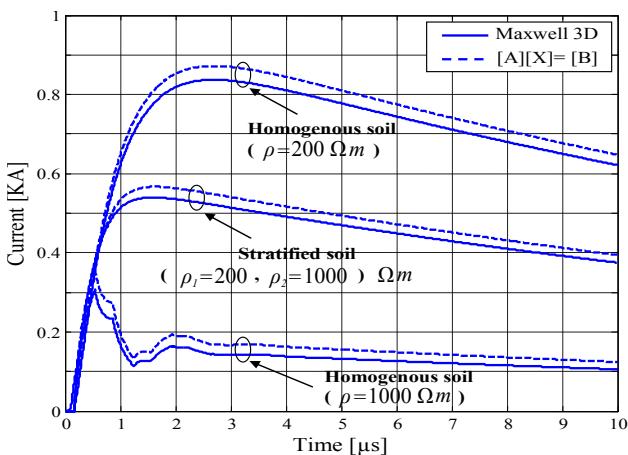


Fig. 11. Time variation of current on the middle of the buried electrode

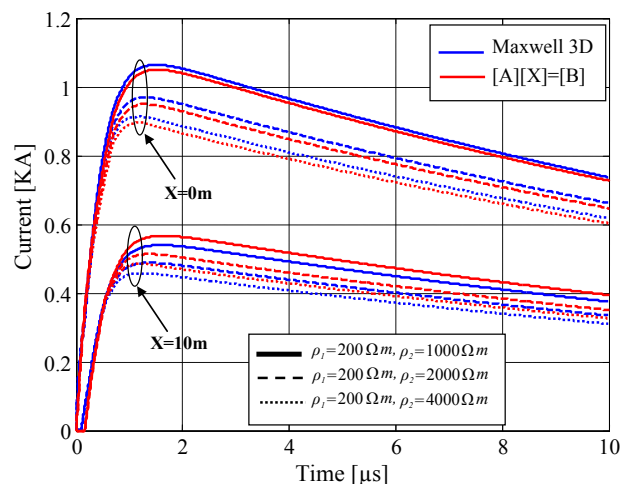


Fig. 12. Temporal variation of current at different points of buried conductor

Next, a parametric study has been undertaken. First, the resistivity of the upper layer is kept constant and the resistivity of the lower layer is varied. Furthermore, the same resistivity of the two layers is assumed while the the burial depth of the horizontal electrode is modified. Influence of the variations in resistivity between the two layers is presented in Figs 12 and 13. In order to confirm the validity of the concept of apparent resistivity, the same electrode is considered. of section *B*. Note that ρ_1 it's the resistivity of the top layer of the finite height h and ρ_2 it's the resistivity of the lower layer of an infinite height. The case of a variation in resistivity between these two layers is considered by assuming two possible scenarios: $\rho_1 < \rho_2$ and $\rho_1 > \rho_2$. First the resistivity $\rho_1 = 200 \Omega m$ of the upper layer is kept constant and the resistivity of the lower layer successively assumes the values $\rho_2 = 1000, 2000$ and $4000 \Omega m$, respec-

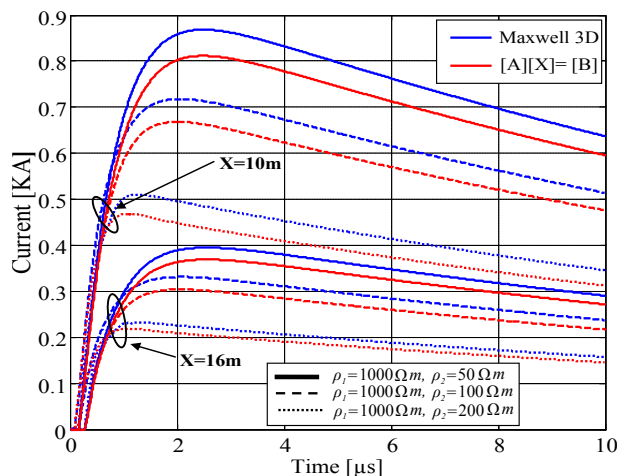


Fig. 13. Temporal variation of current at different points of buried conductor

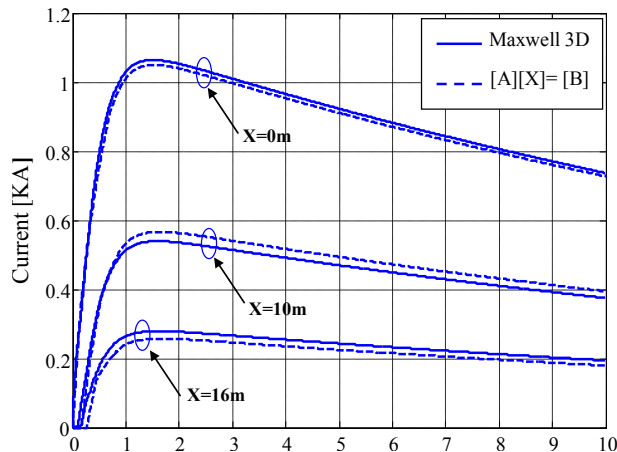


Fig. 14. Temporal variation of current at different points of buried conductor ($h = 0.4m$)

tively. The corresponding transient response is shown in Fig 12.

In the second case the value $\rho_1 = 1000 \Omega m$ is considered while ρ_2 takes successively the values 50, 100 and 200 Ωm , respectively. The corresponding transient response is shown in Fig. 13.

Next set of Figs deals with the influence of the burial depth to the transient response of the horizontal electrode. Figures 14 to 16 show the transient variation of current for different burial depth of the electrode; 0.4, 0.8 and 1.2m respectively.

In part of the spectrum which is of interest for lightning an inductive and capacitive effect, respectively, can be noticed. These effects become less important at low frequency and only a resistive behaviour is dominant, which is visible from figures 11 and 17.

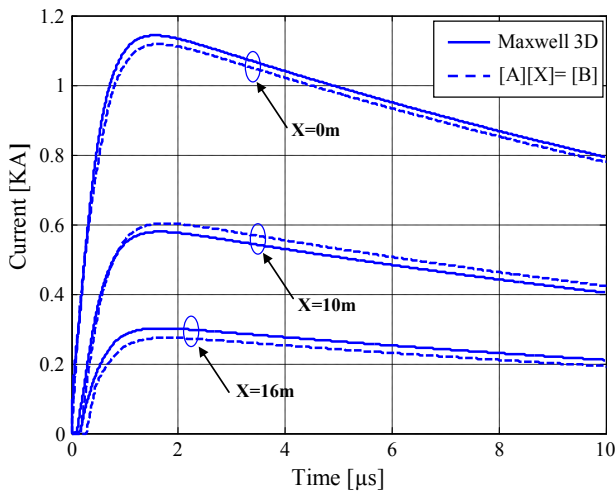


Fig. 15. Temporal variation of current at different points of buried conductor ($h = 0.8m$)

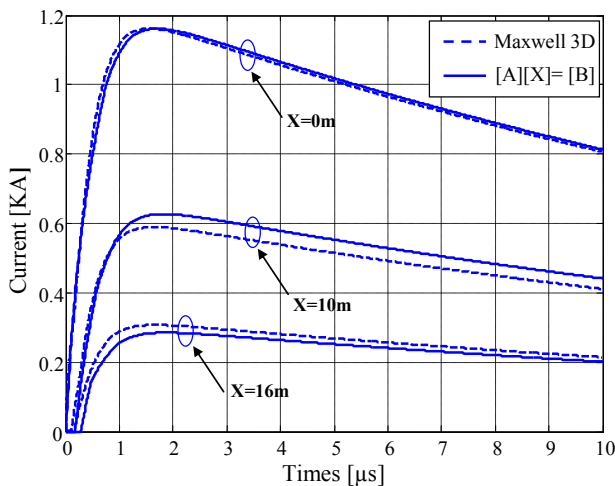


Fig. 16. Temporal variation of current at different points of buried conductor ($h = 1.2m$)

In part of the spectrum which is of interest for lightning an inductive and capacitive effect, respectively, can be noticed. These effects become less important at low frequency and only a resistive behaviour is dominant, which is visible from Figs. 11 and 12.

Table 1 summarizes the results of calculations for the resistance (for $t > 8\mu s$) performed numerically and those obtained analytically by the expressions proposed by E.D. Sunde [6].

7.3 Grounding grid in two-layer stratified soil

In this subsection the case of a grounding grid buried in two layer soil is considered by using the TL approach and the Maxwell's equations approach. Figure 18 shows

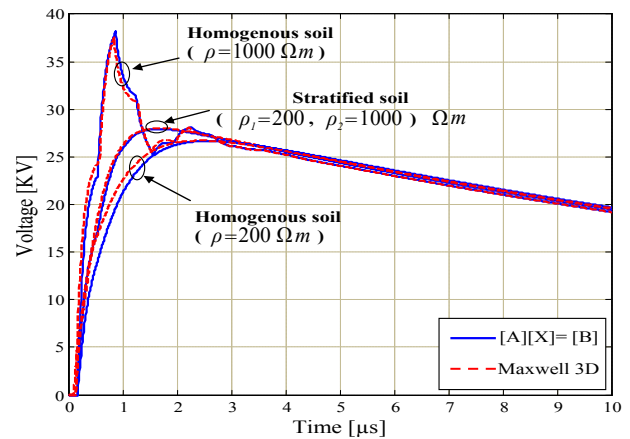


Fig. 17. Time variation of voltage on the middle of the buried conductor

Table 1. Calculation results of the resistance

Resistivity	$\rho = 1000 \Omega m$	$\rho = 200 \Omega m$	$\rho_s = (200, 1000) \Omega m$
Calculation			
Analytical	164 Ω	33 Ω	52 Ω
Numerical	157 Ω	31 Ω	49 Ω
$\frac{\Delta R}{R} \%$	4.20	6.06	5.76

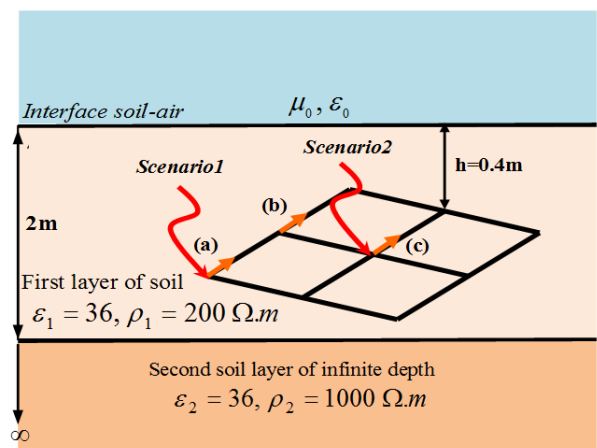


Fig. 18. The horizontal grounding grid in two layer soil

the grid buried at 0.8 m depth in the stratified soil and the size of the grounding grid is 20 m × 20 m. The radius of the conductors is 7 mm and in our simulation, the grounding grid system is excited by double-exponential voltage impulse, $V(t) = 30 (e^{-45099t} - e^{-9022879t})$. Physical constants (ϵ, ρ) of the medium are shown in the Fig. 18.

Two cases are considered, with the injection point on

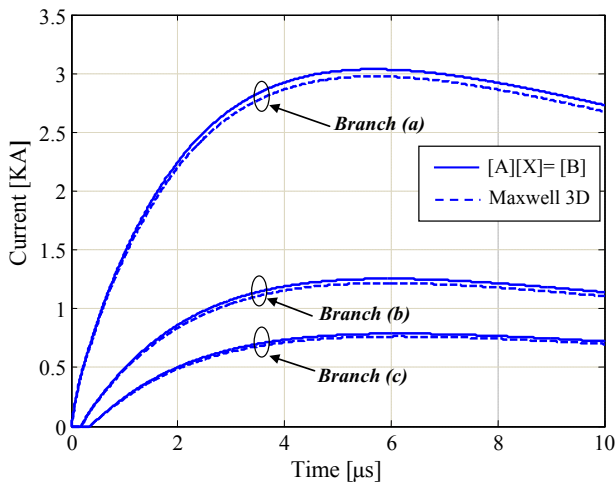


Fig. 19. Transient currents at different points for the horizontal grounding grid

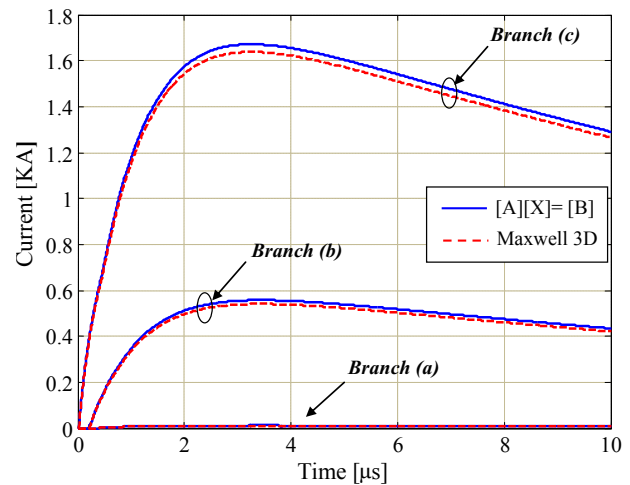


Fig. 21. Transient currents at different points for the horizontal grounding grid

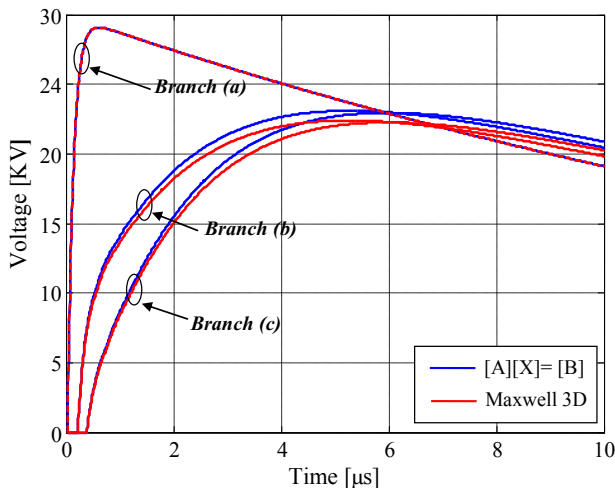


Fig. 20. Transient voltages at different points for the horizontal grounding grid

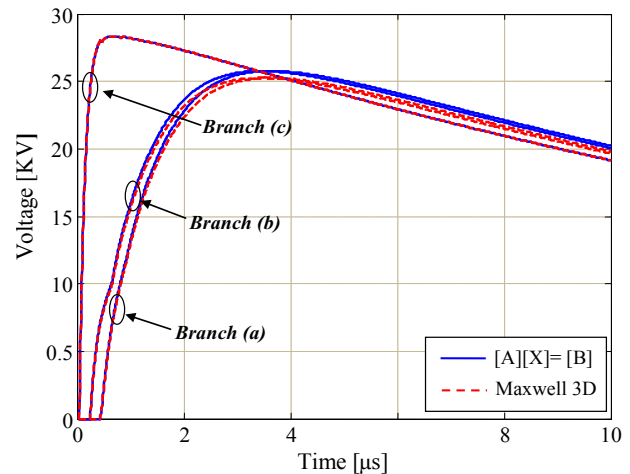


Fig. 22. Transient voltages at different points for the horizontal grounding

the corner and in the middle of the grounding grid system, respectively, as shown in Fig. 18.

Figures 19 to 22 show transient currents and voltages induced on the horizontal grounding grid determined by TL and Maxwell's equations approaches, respectively.

Observing the numerical results obtained by different

approaches presented in figures 19 to 22 agree rather satisfactorily.

It is worth noting that there is a large difference in the computation time required by both approaches on the same machine. For an Intel (R) Core (TM) 2, 1.86 GHz and 0.98 Go of RAM, the results are given in the Table 2.

8 CONCLUSION

The paper deals with two different formalisms for modeling a grounding system excited by a lightning discharge in the presence of multi-layered soils.

For the calculation of currents and voltages distribution using the concept of apparent resistivity it is clear that the TL theory ensures acceptable results. The TL model is

Approach	CPU time consumed
Maxwell 3D	10 hours
[A][X]=[B]	40.44 seconds

simple for implementation and demands a very low computational cost, as it is not required to account for open boundaries. Thus, the principal feature of the method is its simplicity.

On the other hand, the approach related to the solution of Maxwell's equations via the FDTD method provides an advantage of studying the problem directly in the time domain for the layered soil.

REFERENCES

- [1] L. Grcev, F. Dawalibi, "An Electromagnetic Model for Transients in Grounding Systems", IEEE Transactions on Power Delivery, vol. 5, no. 4, pp.1773–1781, November 1990.
- [2] B. Nekhoul, C. Guerin, P. Labie, G. Menier, R. Feuillet and X. Brunotte, "A Finite Element Method for Calculating the Electromagnetic Field Generated by Substation Grounding Systems", IEEE Trans on Magnetic, vol. 11, no. 3, May 1995.
- [3] B. Nekhoul, B. P. Labie, F. X. Zgainski, and G. Meunier, "Calculating the impedance of a grounding system", IEEE Trans. Magn., vol. 32, no. 3, pp. 1509–1512, May 1996.
- [4] K. Tanabe, A. Asakawa, "Computer Analysis of transient Performance of Grounding Grid Element Based on the Finite-Difference Time-Domain Method", Congrès International IEEE-EMC 2003, Istanbul-Turque, 11-16 May 2003.
- [5] B. Harrat, Bachir Nekhoul, Kamal Kerroum, Khalil El Khamlichi Drissi, "A simplified approach to modelling the interaction between grounding grid and lightning stroke". Annals of Telecommunications, vol. 66, no. 11-12, pp. 603–615, November-December 2011.
- [6] E. D. Sunde, "Earth Conducting Effects in Transmission Systems", New York, N. y. Dover publications, inc 1968.
- [7] Y. Liu and al., "An Engineering Model for Transient Analysis of Grounding System Under Strikes: nonuniform transmission-line approach", IEEE Trans. On Power Delivery, vol. 20, pp. 722 – 730, no. 2, April 2005.
- [8] C. R. Paul, "Analysis of Multiconductor Transmission Lines", Wiley Interscience, 1994.
- [9] K. S. Yee, "Numerical Solution of Initial Boundary Value Problems Involving Maxwell's Equations in Isotropic Media", IEEE Trans. Antennas and Propagation, vol. 14, pp. 302–307, 1966.
- [10] K. R. Umashankar, A. Taflove and B. Beker, "Calculation and experimental validation of induced currents on coupled wires in an arbitrary shaped cavity", IEEE Trans. Antennas and Propagation, vol. AP-35, pp. 1248–1257, 1987.
- [11] T. Noda, S. Yokoyama, "Thin wire representation in finite difference time domain surge simulation", IEEE Transactions on Power Delivery, vol. 17, pp. 840–847, no. 3, 2002.
- [12] Y. Baba, N. Nagaoka and A. Ametani, "Modelling of thin wires in a lossy medium for FDTD simulations", IEEE Transactions on Electromagnetic Compatibility, vol. 47, pp. 54–60 no. 1, 2005.
- [13] A. Taflove, K. R. Umshankar and K. S. Yee, " Detailed FDTD Analysis of Electromagnetic Fields Penetration Narrow Slots and Lapped Joints in Thick Conducting Screens", IEEE Trans. Antennas and Propagation, vol. 36, no. 2, pp. 247–257, Feb. 1988.
- [14] A. Taflove, M. E. Brodwin, "Numerical Solution of Steady-State Electromagnetic Scattering Problems using Time-Difference-Dependent Maxwell's Equations". IEEE Trans. On Microwave Theory Tech., vol. MTT-23, pp. 623–630, August 1975.
- [15] Research Project of PEA's Ground Grid in Substation and Grounding in HV and LV Distribution System, Thailand, 2006.



Daoud Sekki was born in 1984 in Jijel, Algeria. He received his BSc and MSc degrees in electrical engineering in 2007 and 2010, respectively, at University of Jijel, Algeria. He is currently preparing his PhD thesis on a topic of electromagnetic compatibility..



Bachir Nekhoul was born in 1957 in Jijel (Algeria). He received his engineering degree in electrical from the National School Polytechnic of Algiers, Algeria, and his PhD at the National Polytechnic Institute of Grenoble, France. He is currently a Professor of Electrical Engineering at the University of Jijel. His scientific research activities concern the electromagnetic compatibility problems. Professor Nekhoul several papers in international journals.



Kamal Kerroum was born in Jijel, Algeria in 1954. He received a state Engineer degree in Electrical Engineering from the Polytechnic School of Algiers in 1978 and a PhD degree in Electrical Engineering in 1981 from the Blaise Pascal University of Clermont Ferrand, France. He is a associate professor at the Institute Pascal of the Blaise Pascal University. His main research areas are Electromagnetic Compatibility, lightning, antennas and propagation and numerical methods in electromagnetics.



Khalil El Khamlichi Drissi received the Diploma Engineer, MSc, and PhD degrees in Electrical Engineering from Ecole Centrale de Lille and the University of Lille, in 1987 and 1990, respectively. He received the Habilitation in electronics, the highest qualification in France at the Doctoral School "Sciences Pour l'Ingénieur" of Blaise Pascal University, in 2001. Dr. El Khamlichi Drissi became Vice President of Research Valorisation, UBP chancellor board in April 2012. Currently, he is a Professor at the

Department of Electrical Engineering, where he was the dean in the period from 2007 to 2011. He is also a senior researcher at the Institut Pascal Laboratory. His research interests include EMC in Power Electronics and Power Systems, in particular: numerical modeling, EMI reduction and converter control. He has been a member of different scientific societies and President of the SEE Auvergne since July 2002 (Society of Electricity, Communication, Electronics and Information Technologies) and Senior Member from December 2, 2003. He has authored or coauthored more than 100 scientific papers published in peer-review journals and presented at international conferences. Dr. El Khamlichi Drissi is a member of IEEE and EEA and has been chairperson and member of scientific committees at international conferences. He is project leader and responsible for several international projects related to EMC (FP7 Marie Curie, Integrafm, Cedre, etc.) and a partner within the Brain City Research Institute. He currently has an on-going collaboration with different companies (IFP, EDF, France Telecom and Landis+Gyr).



Dragan Poljak was born in Split, Croatia in 1965. He received his BSc in 1990, his MSc in 1994 and PhD in electrical engineering in 1996 from the University of Split, Croatia. He is a Full Professor at the Department of Electronics at the University of Split, and he is also an Adjunct Professor at Wessex Institute of Technology. His research interests include frequency and time domain computational methods in electromagnetics, particularly in the numerical modeling of wire antenna structures, and recently numerical modeling applied to environmental aspects of electromagnetic fields.

To this date Professor Poljak has published nearly 200 journal and conference papers in the area of computational electromagnetics, seven authored books and one edited book, by WIT Press, Southampton-Boston, and one book by Wiley, New Jersey. Professor Poljak is a senior member of IEEE, a member of the Editorial Board of the journal *Engineering Analysis with Boundary Elements*, and co-chairman of the WIT International Conference on Computational Methods in Electrical Engineering and Electromagnetics. He is also editor of the WIT Press Series *Advances in Electrical Engineering and Electromagnetics*. In 2004, professor Poljak was awarded by the *National Prize for Science*. He also received *Nikola Tesla award for technical sciences* from the University of Split in 2013.

AUTHORS' ADDRESSES

Daoud Sekki, M.Sc.

Prof. Bachir Nekhou, Ph.D.

Department of Electrical Engineering,

Faculty of Science and Technology,

University of Jijel

Ouled Aissa BP 98, DZ-18000 Jijel, Algeria

email: sekki.daoud@gmail.com, nek_cem@univ-jijel.dz

Assoc. Prof. Kamal Kerroum, Ph.D.

Prof. Khalil El Khamlichi Drissi, Ph.D.

Department of Electrical Engineering,

Institut Pascal,

Blaise Pascal University

Avenue Carnot 34, FR-63037 Clermont-Ferrand, France

email: kamal.kerroum@lasmea.univ-bpclermont.fr,

drissi@lasmea.univ-bpclermont.fr

Prof. Dragan Poljak, Ph.D.

Department of Electronics,

Faculty of Electrical Engineering, Mechanical Engineering

and Naval Architecture,

University of Split

R. Boskovic bb, HR-21000 Split, Croatia

email: dpoljak@fesb.hr

Received: 2013-02-28

Accepted: 2013-10-17